Open Access

SCHOLARENA

Journal of Materials Science and Metallurgy

Non-Linear Elasticity in a Crosslinked Poly-L-(Glutamic acid$_4$, Tyrosine$_1$) Hydrogel

Jorge Monreal*

Department of Physics, University of South Florida, Tampa, Florida, United States of America

***Corresponding Author:** Jorge Monreal, Department of Physics, University of South Florida, Tampa, Florida, United States of America, E-mail: jmonreal@alum.mit.edu

Citation: Jorge Monreal (2024) Non-Linear Elasticity in a Crosslinked Poly-L-(Glutamic acid4, Tyrosine1) Hydrogel, J Mater Sci Metall 5: 101

Abstract

Young's modulii of crosslinked synthetic polypeptide hydrogels have been determined under 75% and 85% relative humidity conditions. Poly-L-(glutamic acid4,tyrosine1) [PLEY (4:1)] was crosslinked with poly-L-lysine (PLK) via 1-ethyl-3-(3-dimethylami nopropyl) carbodiimide hydrochloride (EDC). Elasticity was assessed by subjecting samples to compressive strains. The crosslinked material exhibited non-linear elasticity. Stress-strain response was approximately linear at low strain but nonlinear above a thresh- old strain. Analysis of the secant modulus revealed apparent softening of samples at low strain and hardening at high strain, as in biological soft tissues. Fitting stress-strain data with a neo-Hookean model yielded Young's modulii in the range of approximately $100 \leq E \leq 300$ kPa. There was no statistically significant difference between elasticity of hydrogels at 75% and 85% relative humidities. Here we report results on hydrogels at 75% relative humidity.

Keywords: neo-Hookean; polypeptide; nonlinear

Background

Protein and polypeptide based biomaterials are of increas- ing interest in medicine, biotechnology and biodegradable ma- terials [1, 2]. Advantages of structural proteins for such materi- als include intrinsic biocompatibility and a remarkable range of mechanical properties, for example, high-performance elastic- ity and toughness [1, 2]. Some protein elastomers can withstand over 100 elongation without rupture and return to the original length on removal of stress [3, 4].

Crosslinked polymer networks display non-linear elastic- ity under some conditions. Various theoretical and descriptive models have been proposed. Rubinstein and Panyukov [5], for example, have developed a molecular model of non-linear elas- ticity for entangled polymer networks. Storm et al. [6] have proposed a molecular model of the non-linear elasticity of actin, collagen, fibrin, vimentin and neurofilaments . More recently, Carrillo et al. [7] used a combination of theoretical analysis and molecular dynamics simulations to develop a model of net- worked deformations, which the authors then used to describe non-linear mechanical properties of polymers and biological gel networks. Synthetic polymer networks deform reversibly at an applied stress in the 104 − 107 Pa range. Networks of the proteins actin and collagen, by contrast, deform at stresses as low as 10^{-1}-10^{2} Pa.

Here we assayed the response of crosslinked synthetic polypep- tides to an applied compressive stress. We chose a random co- polymer of L-glutamic acid (E) and L-tyrosine (Y) in a four-to- one molar ratio [PLEY (4:1)]. PLEY molecules were crosslinked with PLK, a polycationic homopolymer, and EDC, a diimide reagent. We compared general trends in the mechanical proper- ties of crosslinked hydrogels with those of biological mateials.

To the author's knowledge, there are no available studies on cross-linked PLEY(4:1) in the field. However, synthetically designed polypeptides are becoming increasingly important in diverse areas such as biodegradable devices, medical implants and mechanical dampers. This study initiates mechanical property studies of materials that have not previously been investigated.

Materials and Methods

Polymers

PLEY (4:1) (MW 20-50 kDa) and PLK (MW 15-30 kDa) were obtained from Sigma-Aldrich (USA). EDC was obtained from TCI America (USA).

Mold

Samples were formed in a custom-made aluminum mold. Fabricated in the USF Department of Physics machine shop, the base and lid of the mold were cut from a 0.5"-thick plate, cylinders were cut into a 0.125"-thick plate, and all flat sur- faces were milled to a roughness of 2.5-25 μm. The mold was designed to produce 1 to 1, length to diameter, cylinders each having a volume of ≈ 50 mm^3. All samples had a nominal di- ameter and height of 4 mm.

Experimental Design

Table 1 summarizes the details of sample composition and humidity conditions. Three experimental factors were the con- centrations of PLEY (4:1), PLK and EDC, and each had three possible values. Relaitve humidity (RH), a fourth factor, also had three possible values. In this study, we used 27 randomized trials as listed in Table S1 of the supplementary material. Table S1 presents the composition of each of the 27 samples as well as RH conditions. Samples variants were fabricated as 3 replicates of 9 different conditions. Not all samples survived processing. Materials were fabricated down the list according to Table S1 so as to not introduce bias. Here we report only on material at RH condition of 75% as there was no statistically significant difference between the two high relative humidity conditions. Materials at 33% RH exhibited nonlinear viscoelasticity and are the subject of a separate report.

Table 1: Experimental factors of this study

Factor	Level		
	-1	**0**	**1**
PLEY (4:1) concentration (% w/v)	30	40	50
PLK concentration (% w/v)	10	15	20
EDC concentration (% w/v)	20 (1.0 M)	30 (1.5 M)	40 (2 M)
Relative Humidity (%)	33	75	85

Materials Fabrication

Equal volumes (40 μL) of PLEY solution, EDC solution and PLK solution were mixed in a 1.5-mL tube using a 250 μL micro-pipette. Volumes delivered were expected to be within 2 μL of nominal, or 5% variation. EDC was mixed first with PLEY to prevent immediate crosslinking. PLK was then added to the PLEY-EDC mixture. Nominal concentrations are listed in Table S1. The molecules contain no chromophores that would allow a more accurate concentration to be determined with UV instruments. Final reaction mixtures were transferred to the mold with a 1-mL syringe and allowed to set up over a 24-h period after which samples were removed from the mold and placed in a humidity chamber. Each sample was allowed to reach humidity equilibrium at 22 oC over a period of 3 days prior to mechanical analysis. Samples that survived processing had diameters of (3.5 ± 0.4) mm and heights of (3.6 ± 0.3) mm.

Humidity Control

Desired RH values were obtained with different saturated aqueous solutions of salt: KCl for 85% and NaCl for 75% [8]. Saturated salt solutions were prepared by adding deionized wa- ter to a minimum of 5 g of salt previously deposited in a 15-mm tall petri dish. Saturated salt solutions were deposited in sepa- rate petri dishes, sealed with parafilm and allowed to reach equi- librium at 22 oC over several days. This method has been shown to provide relative humidities with 2% of nominal values, if pre- pared correctly. Samples removed from the mold were placed in the designated relative humidity chamber according to Table S1.

Materials Testing

Uniaxial compression tests of crosslinked samples were per- formed as illustrated in Figure 1. A digital scale (Centech, USA) with a maximum loading capacity of 1000 g (9.8 N) and a resolution of 0.1 g was placed on top of a lab jack, giving continuous displacement in the vertical dimension. An analog displacement gauge (Pittsburgh Dial Indicator, USA, 0.001 in (0.025 mm) resolution) was used to quantify compression. The sample was placed between the scale and a fixed arm. This sys- tem enabled measurement of spring constants in the 10-1100 N/m range. Displacement was the independent variable; com- pressive force was the dependent variable. A loading curve was obtained for each sample, an unloading curve for selected sam- ples. All data were acquired at 22 oC. Figure S1 in supporting information shows the loading and unloading curve of the ap- paratus itself over the force range of 0.5-6 N.

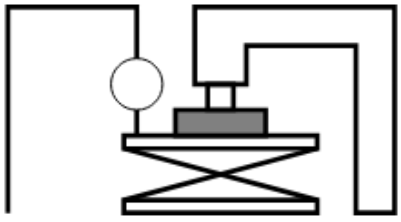

Figure 1: Measurement apparatus. Cylindrical samples were compressed uniaxially along the vertical axis by adjusting the height of the lab jack. Displacement was quantified with a displacement gauge.

Fitting and Parameter Determination

There are several phenomenological models of varying com- plexity that can be used to describe hyperelastic materials. For biological materials and cross-linked polymers, specifically, a neo-Hookean model is widely used. There are some disadvan- tages to the use of a neo-Hookean model. In general, its pre- dictive nature is less accurate than models such as the Mooney- Rivlin, Ogden and Arruda-Boyce models, as examples. Ad- ditionally, the neo-Hookean model does not predict accurately at large strains. However, given that materials in this study showed significant sample to sample variability a neo-Hookean model provided a simple comparative method to discover pat- terns arising from changing experimental conditions. This study did not seek to determine exact values of shear moduli at each given condition. Rather, the aim was to understand changes in elasticity due to changes in condition on a condition-to-condition comparative basis. As an added comparative measure data was also fitted to a two-parameter Mooney-Rivlin model.

All fitting parameters were obtained with MatlabR imple- menting a trust region nonlinear least squares algorithm.

Neo-Hookean Model

Engineering normal stress is $\sigma = F/A_o$, where F is the applied force along a single axis and A_o the original cross- sectional area of the sample. Engineering strain was defined as $\varepsilon = (-\delta)/L_o$, where δ is a compressive displacement and L_o is the original sample length. Principal stretches are defined by engineering strain, $\varepsilon = \lambda - 1$ where $\lambda = (Lo - \delta)/Lo$. For an in- compressible, homogeneous and isotropic material, true stress is

$$\sigma_{true} = \mu\left(\lambda^2 - \frac{1}{\lambda}\right), \tag{1}$$

where $\mu = E/2(1 + \nu)$ is the shear modulus, ν is Poissons ratio, and E is Youngs modulus. The engineering normal stress will be

$$\sigma_{eng} = \mu\left(\lambda - \frac{1}{\lambda^2}\right) \tag{2}$$

on inserting

$$\sigma_{eng} = \sigma_{true}/(1 + \varepsilon). \tag{3}$$

If ν=0.5, as is the case for incompressible isotropic materials undergoing isochoric deformation, then $E = 3\mu$. The neo- Hookean stress model for engineering stress can be fit to stress- strain data to determine μ and thus E.

Mooney-Rivlin Model

The Mooney-Rivlin model used here contains two param- eters. The so-called material constants C_1 and C_2 are here ex- pressed as $\mu_1 = 2C_1$ and $\mu_2 = 2C_2$ to keep notation comparable to that used in the neo-Hookean model. The Mooney-Rivlin model is in essence an extension to the neo-Hookean model.

The engineering normal stress will be

$$\sigma_{eng} = \left(\mu_1 + \frac{\mu_2}{\lambda}\right)\left(\lambda - \frac{1}{\lambda^2}\right) \tag{4}$$

In general, due to our compressive tests we will find negative values of μ_2.

Nonlinear Elasticity Analysis

Many biomaterials display non-linear elasticity [9]. Glan- dular and fibrous breast tissue under compression, for example, displays mostly linear stress-strain curves below 10% strain; a modulus of 28-35 kPa for glandular tissue and about 96-116 kPa for fibrous tissue at 5% strain, and a modulus of 48-66 kPa and 218-244 kPa at 20% strain [10]. Strain stiffening is also displayed by artery walls [11], cornea [12], blood clots [13] and other biological tissues. We found that mechanical proper- ties of crosslinked PLEY material exhibited a similar non-linear behavior as biomaterials under compressive loads.

Force-Displacement Analysis

A force-displacement (F-D) curve such as in Fig. 2 was obtained for each sample. A force reading was recorded after waiting for about 10 seconds at each strain to ensure no re- laxation was evident. No samples at 75% RH (or 85% RH) were found to exhibit time dependence relaxation within the 10 second time period. Loading curves for each of the condi- tions studied here are shown in the supplementary material. The condition label in Fig. 2, 420275, represents 40% (w/v) PLEY, 20% (w/v) PLK, 20% (w/v) EDC and 75% RH. Non-linearity was apparent at higher strains.

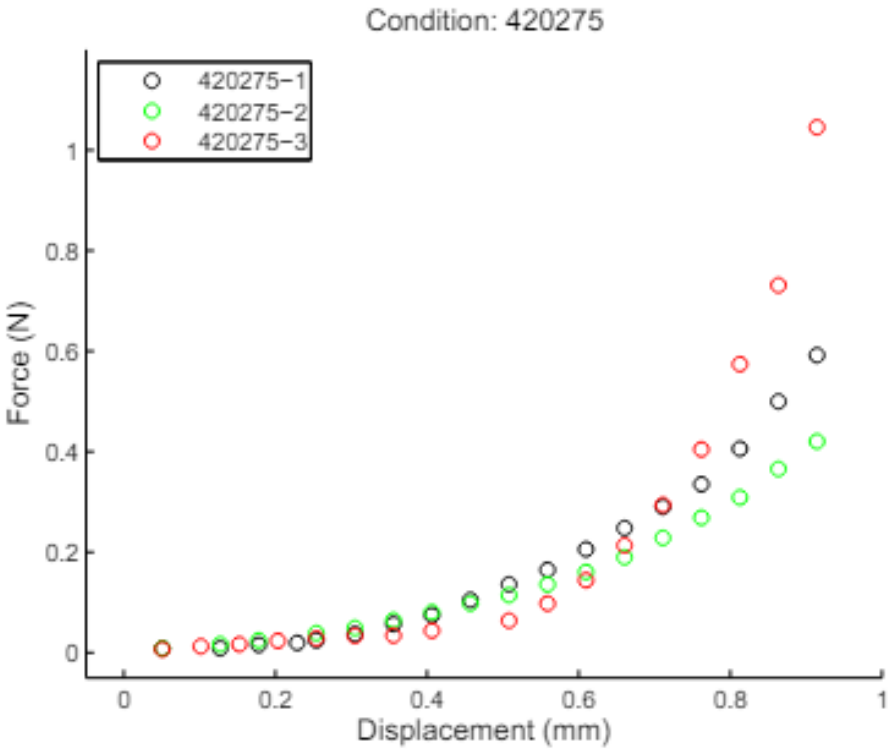

Figure 2: Force-displacement loading curve at 75% relative humidity and 40% w/v nominal PLEY concentration.

Samples for which unloading curves could be obtained with these measurement methods provided initial evidence of non- linear elasticity. Figure 3 shows force-displacement loading and unloading curves for samples at 75%. Circles represent loading, stars un- loading. Loading was clearly non-linear, and unload- ing closely followed loading. This behavior presented initial indications that the material might exhibit non-linear elastic- ity. Such behavior alone might not necessarily indicate non- linear elasticity, howev- er. Further analysis through application of phenomenological models provided additional evidence of non-linear elasticity.

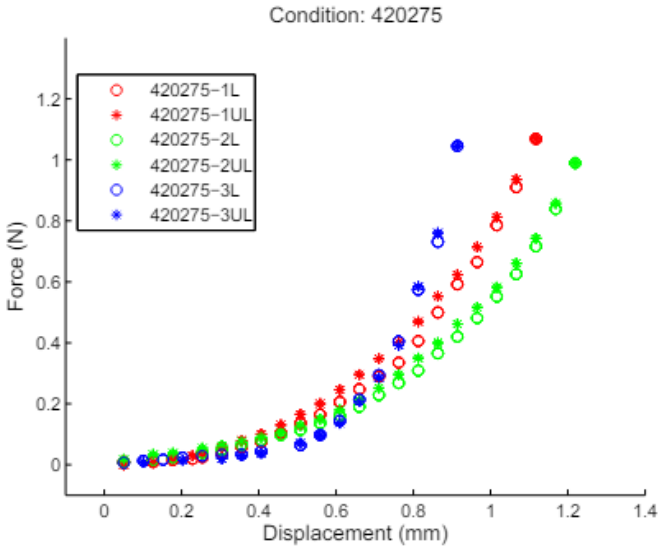

Figure 3: Loading/unloading curves for samples in condition 420275. Specific samples are listed in legend of plot. Circles represent loading; stars, unloading. All three samples show pattern of nonlinear elastic deformation.

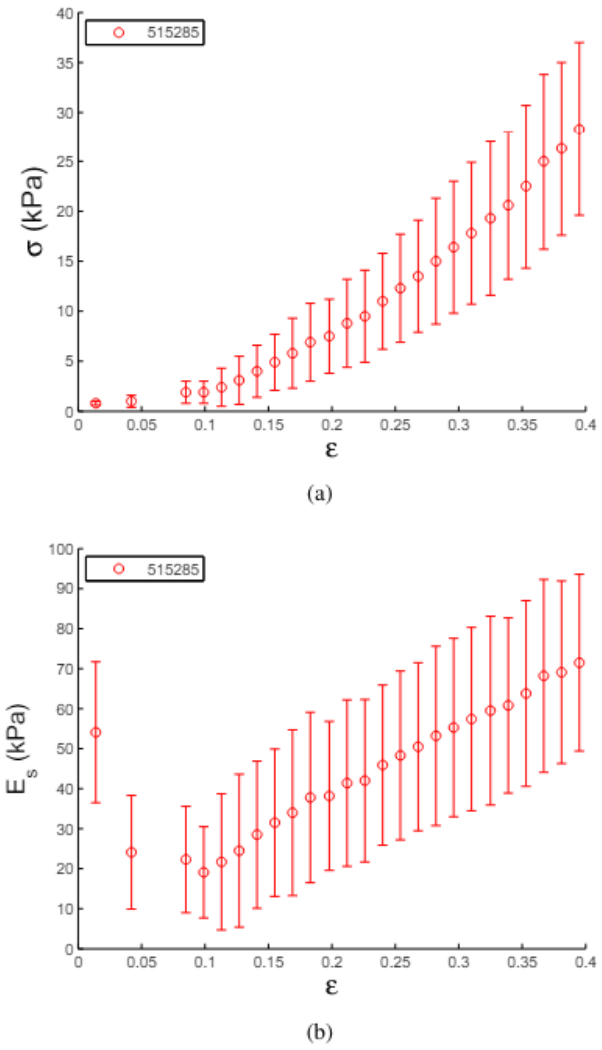

Figure 4: Plots of Stress-Strain and Secant Modulus-Strain curves. Strain- Strain curve exhibits signs of strain hardening at high strain. Secant modulus follows a typical pattern of non-linear elastic biological material. Initial de- crease in secant modulus, then increased secant modulus

with increased strain [14, 15, 16]. (a) Stress versus curve for condition 515285; (b) Secant moduli versus strain curve for condition 515285.

Secant Moduli Analysis

Secant moduli are often used in the analysis of non-linear stress-strain relationships to gain insight on the change in elas- ticity as a function of strain [14, 15, 16]. The secant modulus is approximately the same as the tangent modulus within the linear regime of small deformations, but deviates substantially from the tangent modulus in the non-linear region.

To confirm the mechanical properties of crosslinked PLEY at high RH behaved similar to biological materials, we utilized F-D loading data to generate stress-strain curves and looked for evidence of strain hardening in secant modulus versus strain plots. Figure 4a shows a typical stress-strain curve. Here it is for condition 515285. The secant modulus was evaluated at each data point, i, in the stress-strain curve as

$$(E_s)_i = \frac{\sigma_i}{\varepsilon_i}, \tag{5}$$

where σ_i is engineering stress and ε_i is engineering strain. Fig- ure 4b shows the data of Figure 4a plotted as secant moduli.

Typical curves showed an initial decrease in secant modu- lus at low strain signaling strain softening. For the particular condition presented in 4b strain softening occurred at $\varepsilon < 0.05$. A further load increase resulted in strain hardening. Figure 4b shows strain hardening at $\varepsilon > 0.1$. This analysis provided ev- idence for strain softening at low strains otherwise not notice- able in the stress-strain plot. It also pointed to an inflection of stress at certain strain values, different for each condition, where strain softening transitioned to strain hardening. These results further substantiated the non-linear elasticity of PLEY material. Supplementary material presents secant moduli for all conditions.

Change in Secant Moduli

We were interested in calculating the change in secant mod- ulus at each data point, or the approximate second derivative of stress at each value of strain, to evaluate any further information that could be gleaned from stress-strain data. The change in se- cant modulus was calculated as a modified centered-difference second derivative of the stress with respect to strain at each point:

$$\left.\frac{\mathrm{d}E_i}{\mathrm{d}\varepsilon}\right|_{\varepsilon=\varepsilon_i} = \left.\frac{\mathrm{d}^2\sigma_i}{\mathrm{d}\varepsilon^2}\right|_{\varepsilon=\varepsilon_i} \approx \frac{\sigma_{i+1} - 2\sigma_i + \sigma_{i-1}}{\varepsilon_i^2}. \tag{6}$$

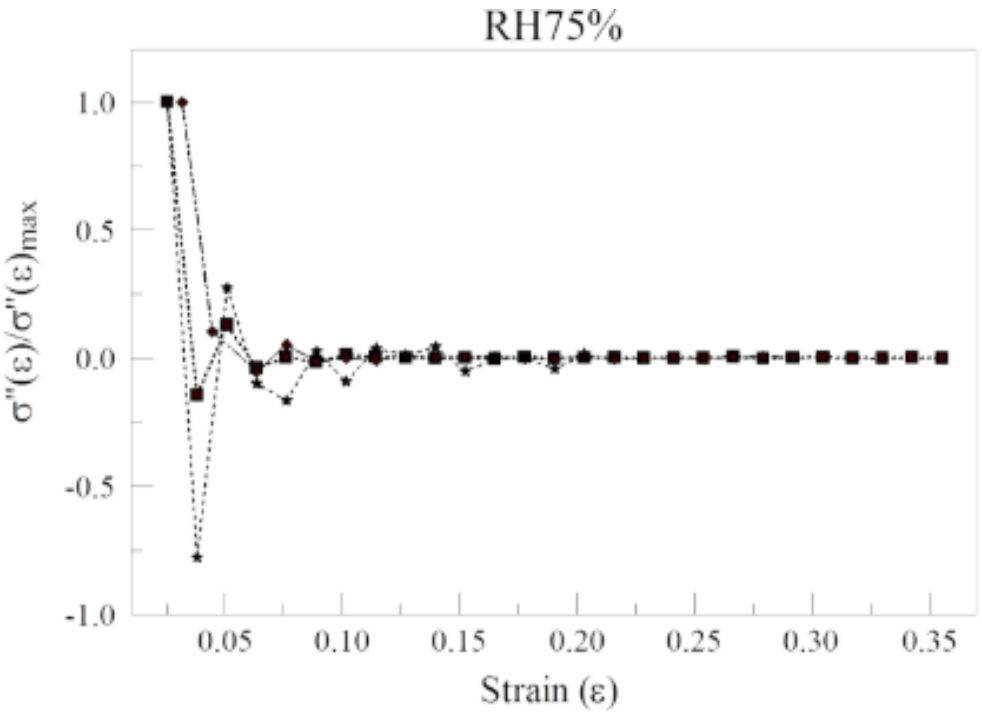

Figure 5: Change in secant modulus. Ratio of change in secant modulus at each strain to maximum change in secant modulus versus strain for 75% RH (Samples: 315375-1; 420275-1; 510475-1).

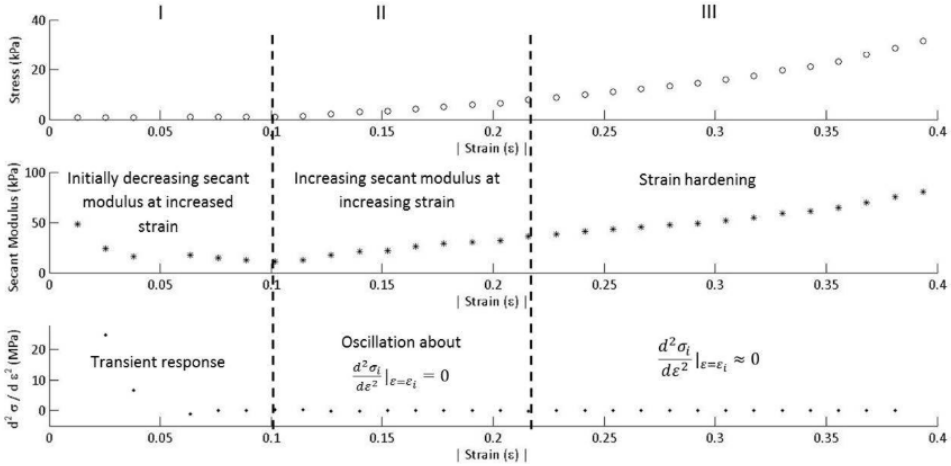

Figure 6: Nonlinear elastic behavior within each of the three regions in stress-strain response of crosslinked synthetic polypeptide co-poly-(L-glutamic acid4, L-tyrosine1). The data are for condition 515285 using sample 515285-3 to show behavioral characteristics within each of the three regions.

The change in secant modulus was found to be analogous to a second-order transient response to an impulse in an electrical circuit. Crosslined PLEY exhibited this type of transient re- sponse at low to medium strain. As strain increased, the change in E_s settled to zero above a certain value of strain, depending on the sample. Figure 5 displays the ordinate axis as the ratio at each value of the strain for samples at 75% RH. One sample from each condition was chosen at random and plotted in this type of plot for presentation only. The interesting behavior calls for additional studies of this type of graphical analysis to be conducted.

$$\frac{\sigma''(\varepsilon)}{\sigma''(\varepsilon)_{max}} = \left.\frac{d^2\sigma_i}{d\varepsilon^2}\right|_{\varepsilon=\varepsilon_i} / \left.\frac{d^2\sigma_i}{d\varepsilon^2}\right|_{\varepsilon=\varepsilon_{max}} \quad (7)$$

$$\left.\frac{d^2\sigma_i}{d\varepsilon^2}\right|_{\varepsilon=\varepsilon_i} \approx 0.$$

Figure 6 compares stress, secant modulus and d2σ/dε2 ver- sus strain for sample 515285-3 (85% RH). The data suggest three distinct regions of response to strain. In the first, the se- cant modulus decreases with increasing strain. This appears to reflect the movement of polypeptide chains relative to each other in a chain re-ordering process. The second derivative dis- plays a transient response in this region. In the second region, there appears to be evidence for the beginning of strain hard- ening evidenced by a damping of oscillatory changes in secant moduli as a response to changes in strain. The second derivative oscillates around zero with a small amplitude, indicating that some of the polypeptide chains are still reordering but others have possibly reached their entropic limit. In the third region,

$$\left.\frac{d^2\sigma_i}{d\varepsilon^2}\right|_{\varepsilon=\varepsilon_i} \approx 0.$$

The secant modulus is increasing in response to increasing strain, indicating a continued but moderate rise in stress at each strain in the stress-strain curve. This region corresponds to strain hardening. Similar behavior is displayed by nonlinear elastic biological materials [15, 16].

Model Fitting

Figure 7 presents stress-stretch data for the condition pre- sented in Figs. 2 and 3. The applied stress was a uniaxial compression. Maximum stretch was 1 for δ = 0. Data are rep- resented by the colored open circles. Equation 2 was globally fit to the experimental data with μ as the fitting parameter and represented by a black line. Youngs modulus was calculated as E = 3μ under the assumption of perfect material incompress- ibility. Table 2 lists shear modulus, μ from a global fit in the second column and calculated Young's Modulus, E, on the third column. The fourth column of table 2 lists the samples at each condition and the fifth column presents shear moduli for each of the samples (see Supplementary Material for plots of individual fits). The last column calculates the standard deviation of shear moduli among samples within each condition.

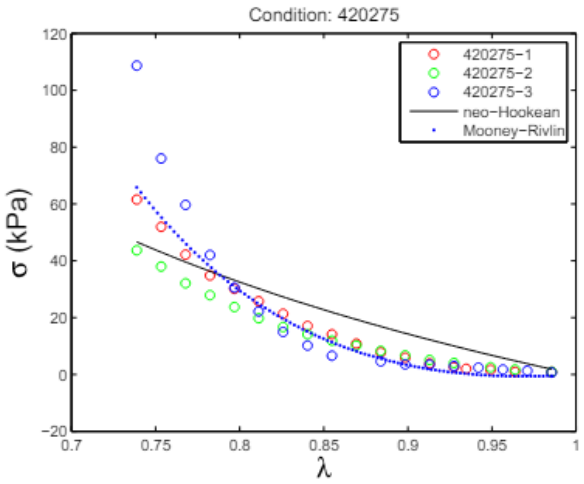

Figure 7: Stress-stretch curves for condition 420275. Determination of stifness parameters with global fitting in MatlabR . Circles represent data values; Solid black line is a global fit with a neo-Hookean model. Blue dotted line is a global fit with a Mooney-Rivlin model. Global and individual values of |μ| are listed in Table 2 for the neo-Hookean model and Table 3 for the Mooney-Rivlin model.

Figure 7 also presents a global fit of data using a two parameter Mooney-Rivlin model, Equation 4, represented by the blue dotted

line. Table 3 lists the fitting parameters from global fits in the second column. The third and fourth columns show samples at each condition with associated fitting parameters from individual fits (see Supplementary Material for plots of individual fits).

Conditions	|μ| (kPa)	E (kPa)	Sample	|μ (kPa)	Std Dev (kPa)
315375	82	246	1 2	102 68	24
420275	43	129	1 2 3	43 33 57	12
510475	40	120	1 2 3	22 57 45	18

Table 2: Youngs moduli values obtained by fitting a neo-Hookean model, $\sigma = \mu(\lambda - 1/\lambda 2)$, to experimental data. First column lists experimental conditions; second lists shear modulus from global fits. E is the Young's modulus. The fourth and fifth columns show samples at each condition with associated shear moduli from individual fits. The last column lists the standard deviation from individual fits (see Supplementary Material for plots of individual fits).

Data in table 2 show larger stiffness occurs at PLEY con- centrations of 30% compared with 50%. We attribute this to a higher degree of crosslinking for lower PLEY concentrations within the range of EDC concentrations used in this study. Higher concentrations of PLEY might not have resulted in additional crosslinking. Rather, unreacted aqueous PLEY, as well as PLK and EDC, probably remained embedded within the crosslinked network leading to lower elastic moduli.

Conditions	[μ1, μ2] (kPa)	Sample	[μ1, μ2] (kPa)
315375	[240, -260]	1 2	[360, -370] [170, -190]
420275	[220, -210]	1 2 3	[170, -170] [90, -100] [470, -420]
510475	[40, -60]	1 2 3	[60, -60] [50, -80] [40, -60]

Table 3: Fitting paramaters obtained by fitting the Mooney-Rivlin model, $\sigma = (\mu 1 + \mu 2/\lambda)(\lambda - 1/\lambda 2)$, to experimental data. First column lists experi- mental conditions; second lists shear moduli from global fits. The third and fourth columns show samples at each condition with associated fitting parameters from individual fits (see Supplementary Matrial for plots of individual fits).

Comparing results of |μ| from global fits of the neo-Hookean model to |μ2| from global fits of the Mooney-Rivlin model we see a similar trend. Conditions at 75% RH decrease for increasing PLEY concentration, with |μ2|=260 kPa for 30% PLEY and |μ2|=60 kPa at 50%. This was not expected.

Conclusion

Due to sample variability values for stiffness here are for comparative purposes only as they relate to trends due to changes in conditions.

We found that trends in mechanical properties exhibited by cross-linked PLEY are similar to those of biomaterials. Load- ing and unloading curves revealed that the polypeptide mate- rials displayed nonlinear elasticity at high relative humidities. Here 75% and 85%. Within a low strain region the material showed signs of strain softening. We attribute this to the begin- ning of polypeptide chain movement and re-orientation relative to each other upon initial compressive loading. As strain increased beyond a certain

value, the material showed signs of strain hardening as evidenced by a secant modulus increase. A plot of secant modulus versus strain clearly showed an inflec- tion point as the material transitioned from strain softening to strain hardening. Plots of change in secant moduli versus strain suggested three regions of stress-strain response in the material. The first region, which included strain softening, seemed to be a trainsient response to strain. The second region showed a damp- ening of oscillatory changes in secant moduli as a response to changes in strain. This can be an indication that some of the polypeptide chains are still reordering but others have possibly reached their entropic limit. This second region seems to be the beginning of strain hardening. Oscillations of the change in se- cant modulii seemed to settle down to zero in the third region. At this region the secant modulii at each strain showed clear signs of strain hardening.

We hope this work opens new areas of research into the en- gineering of designed polypeptides for biomedical applications or applications where biodegradability is desired.

Funding

This research did not receive any specific grant from fund- ing agencies in the public, commercial, or not-for-profit sectors.

Acknowledgments

We would like to thank Donald T. Haynie for very useful comments.

References

1. T. Deming (2012) Topics in Current Chemistry 310.Peptide-Based Materials, Springer-Verlag, Berlin.

2. Q Chen, S Liang G (2013) Thouas, Elastomeric biomaterials for tissue engi- neering, Prog Polym Sci, 38: 584-671.

3. J Gosline, M Lillie, E Carrington, P Guerette, C Ortlepp (2002) Savage, Elastic proteins: biological roles and mechanical properties, Philosophi- cal Transactions of the Royal Society B: Biological Sciences, 357: 121-32.

4. Y Fung (1993) Biomechanics: mechanical properties of living tissues (2nd ed.), Springer-Verlag, New York, NY.

5. M Rubinstein, S Panyukov (2002) Elasticity of Polymer Networks, Macro- molecules, 35: 6670-86.

6. C. Storm, JJ Pastore, FC MacKintosh, TC Lubensky, PA Janmey (2005) Nonlinear elasticity in biological gels, Nature, 435: 1-191.

7. J Carrillo, F MacKintosh, A Dobrynin (2013) Nonlinear Elasticity: From Sin- gle Chain to Networks and Gels, Macromolecules, 46: 3679-92.

8. L. Greenspan, Humidity Fixed Points of Binary Saturated Aqueous Solu- tions, Journal of Research of the National Bureau of Standards-A. Physics and Chemistry 81A.

9. MS Wu, HO (2010) Kirchner, Nonlinear elasticity modeling of biogels, Journal of the Mechanics and Physics of Solids, 58: 300-10.

10. T Krouskop, TM Wheeler, F Kallel, BS Garra, T Hall (1998) Elastic Moduli of Breast and Prostate Tissues Under Compression, Ultrasonic Imaging 0, 260-74.

11. RE Shadwick (1999) Mechanical design in arteries, J. Exp. Biol 202: 3305–13.

12. J Hjortdal (1995) Extensibility of the normo-hydrated human cornea, Acta Oph- thalmol. Scand, 73: 121-71.

13. JV Shah, PA Janmey (1997) Strain hardening of fibrin gels and plasma clots, Rheologica Acta, 36: 262-8.

14. DV Rosato, DP DiMattia, DV Rosato (1991) Designing with Plastics and Composites: A Handbook, Van Nostrand Reinhold, New York, NY.

15. JP Mills, L Qie, M Dao, CT Lim, S Suresh (2004) Nonlinear Elastic and Viscoelastic Deformation of the Human Red Blood Cell with Opti- cal Tweezers, Molecular and Cellular Biology, 42: 169-80.

16. O. Chaudhuri, S Parekh D (2007) Fletcher, Reversible stress softening of actin networks, Nature, 445: 295-8.